NASA TECHNICAL NOTE

NASA TN D-4892

NASA TN D-4892

ROTATIONAL AND VIBRATIONAL TEMPERATURE MEASUREMENTS IN THE 12-INCH HYPERSONIC CERAMIC-HEATED TUNNEL

by John C. Hoppe

Langley Research Center

Langley Station, Hampton, Va.

NATIONAL AERONAUTICS AND SPACE ADMINISTRATION • WASHINGTON, D. C. • NOVEMBER 1968

NASA TN D-4892

ROTATIONAL AND VIBRATIONAL TEMPERATURE MEASUREMENTS IN THE 12-INCH HYPERSONIC CERAMIC-HEATED TUNNEL

By John C. Hoppe

Langley Research Center
Langley Station, Hampton, Va.

NATIONAL AERONAUTICS AND SPACE ADMINISTRATION

For sale by the Clearinghouse for Federal Scientific and Technical Information
Springfield, Virginia 22151 – CFSTI price $3.00

ROTATIONAL AND VIBRATIONAL TEMPERATURE MEASUREMENTS IN THE 12-INCH HYPERSONIC CERAMIC-HEATED TUNNEL

By John C. Hoppe
Langley Research Center

SUMMARY

An electron-beam fluorescence technique has been employed to measure free-stream nitrogen rotational and vibrational temperatures in air at the Langley 12-inch hypersonic ceramic-heated tunnel. This work included establishing the sources of measurement uncertainty and minimizing their effect on the temperature measurements. An extensive laboratory study to determine the accuracy of the instrument system preceded tests made at the facility.

Measurements obtained at the facility included a rotational temperature range from 39° K to 72° K and a corresponding vibrational temperature range from 850° K to 1320° K. In addition, static translational temperatures were determined as well as the condition of nonequilibrium existing in the gas expansion. Uncertainties in these measured temperatures are estimated to be ± 5 to ± 7 percent for the rotational temperatures, and ± 15 percent for the vibrational temperatures. Contributing factors are discussed in the text of the report. During the preliminary laboratory investigation of the technique for vibrational temperature measurement, experimental evidence indicated that at least one reported transition probability needed correction. In addition, some deviation from the expected linear analysis for rotational temperature was experienced. Finally, the measured temperatures generally agree with aerodynamic predictions and fall between the extreme frozen flow and equilibrium flow cases. A first-order nonequilibrium theory fits the observations approximately.

INTRODUCTION

The ability to measure accurately the local free-stream gas temperature and density in low-density hypersonic facilities would substantially improve the quality of research data obtained in these facilities. An electron-beam fluorescence technique has proven to be very useful to this end. Previous work (refs. 1 to 5) indicates the utility of such a technique in low-density hypersonic airstreams. Principally developed by E. P. Muntz (ref. 1), the general method involves spectroscopic analysis of electron-produced fluorescence. Light is emitted by test gas molecules excited in the vicinity of

a collimated beam of electrons. The electron energy is moderate, about 10 to 30 keV. The intensity distribution of the light from excited molecules can then be related to microscopic properties, for example, temperature and density.

The purpose of this paper is to report and discuss the use of the electron-beam technique to measure molecular rotational and vibrational temperatures of N_2 in a hypersonic tunnel employing air as a test gas. The present investigation involves work with the measurement technique in both the laboratory and in a Mach 13 hypersonic test facility. In order to determine and minimize the measurement uncertainty of this technique, an extensive exploratory study was conducted under controlled laboratory conditions. Pertinent results from the laboratory work are reported.

SYMBOLS

A	nozzle exit area, meters^2
A^*	nozzle throat orifice area, meters^2
B_O	rotational constant, for lowest vibrational energy level (ref. 12), centimeter^{-1}
$B^2\Sigma_u^+$	B excited electronic state for molecules
c	velocity of light, meters/second
E_K	Kth rotational level energy value, centimeter^{-1}
f_r	function symbol, rotational temperature
f_v	function symbol, vibrational temperature
$G_O(x)$	vibrational energy, relative to ground-state value, of x vibrational level, centimeter^{-1}
h	Planck's constant
I	relative intensity
k	Boltzmann's constant
K'	rotational quantum number for $N_2^+B^2\Sigma_u^+$

K_1''	rotational quantum number for $N_2X^1\Sigma_g^+$
K_2''	rotational quantum number for $N_2^+X^2\Sigma_g^+$
N_2	diatomic nitrogen
N_2^+	singly ionized diatomic nitrogen
$p(\ ,\ )$	vibrational transition probability
p_o	stagnation pressure, newtons/meter^2
r	throat radius of hypersonic nozzle, meters
T	temperature, degrees Kelvin
T_o	stagnation temperature, degrees Kelvin
T_r	molecular rotational temperature, degrees Kelvin
T_v	molecular vibrational temperature, degrees Kelvin
T_∞	free-stream static translational temperature, degrees Kelvin
V	gas velocity, meters/second
v'	vibrational quantum number, $N_2^+B^2\Sigma_u^+$
v_1''	vibrational quantum number, $N_2X^1\Sigma_g^+$
v_2''	vibrational quantum number, $N_2^+X^2\Sigma_g^+$
$X^1\Sigma_g^+, X^2\Sigma_g^+$	X ground electronic states for molecules
α	half-angle of conical hypersonic nozzle, radians
λ	wavelength, angstrons (Å)
ν	wave number
ρ	mass density, kg/m^3

$\sigma(T)$ vibrational energy of N_2 at free-stream vibrational temperature T, centimeter^{-1}

$\sigma(T_o)$ vibrational energy of N_2 at stagnation temperature T_o, centimeter^{-1}

$\chi(K', T_r)$ function characteristic to rotational temperature analysis, specified in references

Subscripts:

a used to differentiate between two vibrational states

o stagnation conditions, referenced to lowest energy

r rotational energy states

ref reference value

v vibrational energy states

1 refers to $N_2 X^1\Sigma_g^+$ state

2 refers to $N_2^+ X^2\Sigma_g^+$ state

∞ refers to free-stream static conditions

MEASUREMENT TECHNIQUE

To describe briefly the character of the electron-beam technique without elaborating on the theory in detail, figure 1 illustrates the nitrogen energy level scheme and the physical process. The "fast" electrons (28 keV) interact with the $N_2^+ X^1\Sigma_g^+$ ground-state molecules, exciting and ionizing some directly to the intermediate $N_2^+ B^2\Sigma_u^+$ state. Excited B state molecules decay in about 10^{-7} seconds (ref. 6) to the stable ion ground state $N_2^+ X^2\Sigma_g^+$ by spontaneous photon emission. Vibrational bands (labeled v', v_2'') and within them rotational lines (labeled K', K_2'') characteristic of molecular spectra, are found to compose this emission. Details of the theoretical work, such as applicable selection rules on the excitation and emission processes, spectroscopic notations, and other features may be found in references 1, 4, 5, 7, and 8.

The temperatures of importance here, rotational T_r and vibrational T_v, are determined by means of spectrometric intensity analysis of the rotational lines and vibrational bands, respectively. The analyses are outlined by the expression:

$$T_v = f_v\left[\frac{I_{band}(v')}{I_{band}(v'_a)}\right] \qquad (v' \neq v'_a)$$

for the respective upper levels of vibrational transition intensities $I_{band}(v')$, and

$$T_r = f_r\left[\frac{I_{line}(K')}{I_{ref}}\right]$$

for rotational line intensities $I_{line}(K')$. The absence of any vibrational designation in T_r is to be taken to mean rotational intensities for a single v', v''_2 transition in $N_2^+\left(B^2\Sigma_u^+ - X^2\Sigma_g^+\right)$. Explication of the equations for temperature will follow in later sections. Additionally, the translational temperature can be considered as equal to the rotational because of the very rapid relaxation of translational and rotational energies (refs. 9 and 10). Hence, in a nozzle expansion, such as occurs in the Langley 12-inch hypersonic ceramic-heated tunnel, rotational and translational motion have established an equilibrium between themselves very quickly $(\approx 10^{-10}$ sec). Then, the three characteristic temperatures can be determined by using the electron-beam method.

APPARATUS

Essential instrumentation to perform the temperature measurements consisted of the electron gun (beam source), spectrographic dispersing and detection elements, and readout equipment. The basic elements of the electron gun are shown in figure 2. The anode chamber accelerates the electrons produced from the filament. Focus coils collimate the stream to allow it to pass through a drift tube, and finally exit through a 1.02×10^{-3} m (0.040 in.) aperture. Operating pressures below 1.33×10^{-2} N/m^2 $(10^{-4}$ torr) are required within the gun chamber. As illustrated, the assembly was operated without multiple pressure staging, since external pressures were sufficiently low in the Langley 12-inch hypersonic ceramic-heated tunnel. Nominal operating parameters for the beam were a potential of 28 kV and actual currents in the test region of 0.6 to 1 milliampere.

The placement of the gun and spectrometric instrumentation in the tunnel test section is diagramed in figure 3. An end view simply illustrates the center-line position and vertical direction of the electron beam. It also indicates the manner of viewing the

fluorescence through the side ports. A side view is shown to demonstrate completely the overall instrument placement. The exit orifice of the gun was placed as far into the test section as practical, interruption of the flow being avoided. A manually operated gate valve was placed on the end of the drift tube. It was operated during intervals of high pressure in the test section to prevent overpressure in the gun. The element of fluorescence observed by the two scanning spectrometers, one on each side of the tunnel, occurred at a point 5.1×10^{-2} m (2 in.) downstream of the hypersonic nozzle exit. That arrangement placed the test gas element 1.12 m (44 in.) from the throat of the nozzle and about 2.3×10^{-1} m (9 in.) from the orifice at the end of the electron gun drift tube. From the data in reference 11, a pitot rake at the same position as the observed volume of gas indicates an effective test core size of about 1.5×10^{-1} m (6 in.) diameter for a Mach number of about 13. These values are for typical tunnel operating conditions. As pointed out, the observations were made at the tunnel center line (vertical and horizontal). With the 1.02×10^{-3} m gun exit as close as possible to the test volume, beam spreading was thus minimized.

Continuous monitoring of the beam current during tunnel runs was an important feature. Figure 2 also shows the method of measurement. The tunnel itself provided the collector. The current was read by means of ground return, through a picoammeter connected directly to a strip chart recorder, to the high voltage supply. Relatively long tunnel run times (45 to 80 seconds) allowed the use of such a low response system (1 second).

Since two ports were available for viewing the fluorescence of the beam, two spectrometers were utilized for most of the investigation. (Some of the time density measurements were conducted by leaving only one port to provide temperature data.) The spectrometers were 0.5-meter focal length instruments with 64 mm × 64 mm gratings and 1200 grooves/mm; one was blazed at 4000 Å and the other, at 3000 Å. The former spectrometer was used for vibrational band measurements and the latter spectrometer, for rotational line measurements. Reciprocal dispersion was 16 Å/mm and resolution, for conditions of a 1 centimeter slit height and 10 μm (10 micron) slit width, was better than 0.1 Å. Actual slit widths used were 25 μm (25 microns) for rotational measurements, which was sufficient to resolve the R-branch lines in $N_2^+\left(B^2\Sigma_u^+ - X^2\Sigma_g^+\right)$ bands, and 250 μm (250 microns) for vibrational measurements to provide the band profiles. Each band is composed of two branches designated P and R branches.

With a lens sufficient to fill the solid angle of the spectrometer in each case, that is, f/5 where f is the ratio of focal length to diameter, magnification was found to be about 0.5. The observed fluorescence then emanates from a segment of beam which is physically twice the slit dimension. Therefore, the measurements represent effectively an average over a corresponding volume of gas, when a beam diameter of about 1×10^{-3} m

(1 mm) is considered. The lenses used were optical-grade quartz, as were the port windows on the tunnel and the photomultiplier face windows; therefore, uniform transmission throughout the wavelength range was insured.

The detection element for each optical system was provided by a thirteen-stage photomultiplier tube, S-13 response, operated in the linear range at a gain of about 3×10^7. Signal-noise ratios were kept large enough to provide good data throughout the work. A better indication of that condition is provided later with the error analyses. The detected signals were read out through picoammeters connected to 0.25-second strip-chart recorders.

Lastly, the rate of scan for the spectrometers is of importance. The scan rate was selected for compatibility with the recorder response on the basis of the spectrometer slit width and the desired wavelength interval. This adjustment eliminated superfluous effects, such as signal attentuation. The optimum scan was used in each of the two cases so that rotational spectra generally were recorded in about 12 to 15 seconds. The vibrational scan involved a larger wavelength interval and required about 30 seconds per measurement. In the course of a tunnel run, one to five individual rotational and one or two vibrational scans were possible. Figure 4(a) shows vibrational data typical for a single tunnel run.

DATA ANALYSIS

Vibrational Temperature

In discussing the derivation of temperatures from the intensity data, only the pertinent points in theoretical approach and the practical aspects are treated. The earlier references provide the background underlying the following procedures. The vibrational spectra of figure 4 are utilized as the present example. In extent and form the 0,1 and 1,2 recorded band shapes of the $N_2^+\left(B^2\Sigma_u^+ - X^2\Sigma_g^+\right)$ transition are determined by the rotational temperature, the scan rate (125 Å/min) and the spectral resolution. A 250 μm (250 micron) slit width was effectively 4 Å wide at the spectrometer exit slit, for this particular instrument.

The method of acquiring the band intensity ratio experimentally was most important. There were several possible approaches which could be employed (see refs. 12 to 14), although here only two of the simpler ones are discussed. The important feature for each of these two methods is a complete separation of bands. Figure 4(a) illustrates that such separation occurs when the rotational temperature is sufficiently low and where there is a reasonable wavelength interval between the band heads (here $\approx$40Å). The first technique follows, since in such a case mechanical integration of the area under a profile is one straightforward determination of I_{v',v''_2}. However, to effect the second procedure,

advantage may be taken of particular circumstances, where the P branches of two useful bands contain the same number of lines and approximately the same spectral extent. Then, in the case of some $N_2^+\left(B^2\Sigma_u^+ - X^2\Sigma_g^+\right)$ bands, the proper slit width allows the peak of the P branch profile to represent the relative band strength. Hence, the ratio of the peaks for the 0,1 and 1,2 bands is essentially the intensity ratio. For all measurements conducted in the ceramic-heated tunnel, the second method discussed served to obtain the vibrational intensity ratio. The remaining step to find the vibrational temperature is to compare the experimental ratio with its calculated dependence on temperature.

That these methods are workable was investigated in a laboratory study prior to field application; figure 4(b) is an example. Figure 5 shows a comparison of some of the laboratory data with the theoretical temperature dependence; this comparison covers a reference temperature range of 300° K to 1000° K. However, where the gas temperature becomes greater than about 400° K in the laboratory work, band overlap becomes a significant error source. Then, an empirical correction was utilized for the band profile integration technique of determining the intensity ratio. By further laboratory work and calculations of such an overlapped condition, the 10 percent and larger uncertainty introduced while empirically correcting this condition could probably be improved. Figure 4(b) illustrates the overlap at higher rotational temperature and the correction. A more extensive discussion of the various sources of error follows the results. In the laboratory work, only at 300° K could the P branch peak values be utilized to check the validity of using peak values. However, the very good agreement of all methods, among themselves and with theory, at that temperature shows that they are applicable.

As indicated previously, measured vibrational temperatures for the free stream of the Langley 12-inch hypersonic ceramic-heated tunnel were 850° K to 1320° K. For the entire set of data, the ratio $I_{0,1}/I_{1,2}$ $\left(0,1 \text{ and } 1,2 \text{ bands of } N_2^+\left(B^2\Sigma_u^+ - X^2\Sigma_g^+\right)\right)$ was utilized. It is the most sensitive ratio up to about 2500° K, and retains such useful features as adjacent bands to minimize the vibrational scan time. For comparison, two other ratios are shown in figure 6 as functions of temperature, $I_{0,0}/I_{1,1}$ and $I_{0,2}/I_{1,3}$.

The relative transition probabilities $p\left(v', v_2''\right)$ (reference the v', v_2'' designation of vibrational transitions in fig. 1) are very important in determining the ratios. Theoretical intensity-temperature relations have the form

$$\frac{I_{v', v_2''}}{I_{v_a', v_{2a}''}} = \left(\frac{\lambda_a}{\lambda}\right)^4 \frac{p\left(v', v_2''\right)}{p\left(v_a', v_{2a}''\right)} \frac{\sum_{v_1''} \left[p\left(v', v_1''\right) e^{-G_o\left(v_1''\right)hc/kT_v}\right]}{\sum_{v_1''} \left[p\left(v_a', v_1''\right) e^{-G_o\left(v_1''\right)hc/kT_v}\right]} \qquad \left(v_a' \neq v'\right)$$

where λ represents the wavelength of the band and T_v, the vibrational temperature. The vibrational energy of the v_1'' state is $G_o(v_1'')$ and the constants are h, c, and k. Uncertainty in the probabilities contributes directly to the temperature uncertainty where the intensity ratio obtained experimentally is compared to find T_v. The values of $p(v',v_2'')$ used in this work appear in table I. They are the same as in table I of reference 1 except p(1,3). Additional information concerning the transition probabilities can be obtained from reference 15. Although they represent perhaps the best to date, there is still some discrepancy. Two values were found to be quoted twice in references 1 and 15 with different values. Those in the table were chosen to give consistent results based upon the laboratory work. Also, the present value 0.16 given for p(1,3) differs considerably from 0.26 of references 1 and 15. Figure 6 shows data to support the smaller number. The value p(1,3) = 0.16 is derived completely on an experimental basis $(I_{0,2}/I_{1,3}$ data).

TABLE I

RELATIVE TRANSITION PROBABILITIES $p(v',v_2'')$ FOR SOME VIBRATIONAL BANDS IN THE $N_2^+(B^2\Sigma_u^+(v') \rightarrow X^2\Sigma_g^+(v_2''))$ ELECTRONIC TRANSITION

v'	Transition probabilities for v_2'' of –			
	0	1	2	3
0	0.54	0.23*	0.07	0.02
1	.21	.27	.27*	.16**
2	.04	.29	.06	.23

*Quoted in references 1 and 15 with different values.

**Value based on present experiments.

Another very significant factor in the analysis is the correction for photomultiplier sensitivity variations with wavelength. This correction, of course, enters these decisions about $p(v',v_2'')$ as well. A standard of spectral radiance, a precalibrated tungsten filament lamp, was used to determine directly the overall relative sensitivity of the spectrometer and phototube system as a function of wavelength. The optical arrangement was such as to simulate closely the intensities provided by the electron beam fluorescence at appropriate wavelengths. The uncertainty in the calibration is much less than that estimated for the probabilities, as is seen later. Such a condition should exist in order to estimate reasonably a given $p(v',v_2'')$. To correct the difference in relative sensitivity between the 0,1 and 1,2 bands, the directly calculated $I_{0,1}/I_{1,2}$ value is multiplied by 0.97.

With this additional correction between 0,1 at 4278 Å and 1,2 at 4235 Å, a final ratio such as that determined by the peaks in figure 4(a) can be used to obtain the vibrational temperature. That particular point appears in figure 5 at $\approx 900^{\circ}$ K. All the results from the Langley 12-inch hypersonic ceramic-heated tunnel were obtained by utilizing the peak values of the 0,1 and 1,2 P branch profiles. Several of the spectra were integrated mechanically as well to provide a comparison between the two techniques. In those particular cases, agreement was found between vibrational temperatures determined by using peak ratios and from the integrated values.

Rotational Temperature

Determination of the nitrogen rotational temperature requires evaluation of individual line intensities in the $N_2^+\left(B^2\Sigma_u^+ - X^2\Sigma_g^+\right)$ bands. Since the 0,0 band is the strongest of the system its use is preferable. The 25 μm slit width resolved the R-branch lines in that band, as figure 7 shows. Although rotational measurements are possible without this resolution (see, for instance, ref. 16), it provides a straightforward approach. The traces in figure 7 are representative of the data obtained in the Langley 12-inch hypersonic ceramic-heated tunnel. The appearance of only a few lines indicates the low rotational temperature condition.

It is perhaps well to indicate a more specific form of the general temperature equation which appeared in the Introduction. Attention is called to the articles of Muntz, Sebacher and Duckett, Petrie, et al., or Hunter (refs. 1, 2, 4 or 5) for the details. The R-branch line intensities are related to the rotational temperature through a somewhat altered Boltzmann form. This alteration reflects the excitation and ionization path (through selection rules), and leads to the form

$$-\log_e\left[\frac{I_{K'}}{I_{ref}}\frac{1}{\chi\left(K', T_r\right)}\right] = \frac{E_{K'}}{kT_r}$$

where $I_{K'}$ and $E_{K'}$ are the $K'K_2''$ line intensity (see fig. 1) and upper K' level's energy, respectively. The factor $\chi\left(T_r, K'\right)$, specified in the references (refs. 1 or 5) accounts for the pertinent selection rules, excitation path, and hence, the slight deviation from a strictly Boltzmann form. The term T_r, of course, refers to the ground-state-neutral N_2 molecules, which are assumed to have a Boltzmann energy distribution. The χ factor also includes constants for the band, and because of its dependence on temperature, requires an iterative procedure to solve the equation.

An expression for the rotational energy is $E_{K'} = B_0 hc\left[K'(K' + 1)\right]$, B_0 being a rotational constant. This representation neglects small corrections due to populating higher vibrational levels initially, or higher vibrational temperature, and $\left[K'(K' + 1)\right]^2$

terms, which are significant only at high K'. (See ref. 8.) A rotational temperature may be obtained by a graphical analysis with the logarithm expression as a function of $K'(K' + 1)$. A straight line should be obtained and from it the temperature T_r is found by

$$\text{Measured slope} = \frac{B_0 hc}{kT_r}$$

This method is the simplest one, particular refinements being made to suit the needs. In the present case, for example, a least-squares analysis was incorporated and the necessary iterative procedure was carried out with a computer. Figure 8 presents the graphical representation of one resultant straight line obtained by a least-squares fit.

In the continuation of the explanation of the analytical procedure, attention is called once more to the spectra shown in figure 7. By using only those lines with K' being odd integer values, about five points were available for the $-\log_e\left[\frac{I_{K'}}{I_{ref}} \frac{1}{\chi(K', T_r)}\right]$ evaluation as a function of $K'(K' + 1)$. The use of only K' even or K' odd is necessary because the lines are weighted by nuclear spin, K' odd being about twice the intensity of K' even. A rapid scan ($\approx$50 Å/min) caused the rather narrow structure of the recorded spectrum. This spectrum with some noise being present at the useful sensitivities requires a statistical analysis to obtain the best value for the slope. Use was made of a least-squares straight-line fit with weighting factors based on a standard deviation due to noise (ref. 17, for instance). Weighting factors were determined experimentally from both tunnel data and in the static test chamber in the laboratory, where the light levels were controlled to approximate the tunnel data.

The straight line, such as in figure 8, and hence the slope were determined by computer program, by utilizing these methods. A knowledge of the approximate temperature range, from reference 11, and the initial tunnel data demonstrated that only a small range of rotational temperatures (40° K to 75° K) would be encountered. It was, therefore, easy to program an iteration over the entire range in 5° K steps. A free-stream temperature could be calculated to within approximately 0.3° K. That value was considered to be satisfactory because the approximations of the method and the experimental uncertainties contribute larger errors.

Although the uncertainties are evaluated subsequently, some discussion of the approximations may serve here. In particular, figure 9 demonstrates some of the data in which noticeable curvature of the points appeared. At the highest stagnation temperatures, no such bending appeared. However, at the lowest stagnation temperature condition, some small amount was detected consistently. Several features of the technique were considered in attempting to establish the cause.

Instrumentation was eliminated as the source of curvature. It was found that the data points were very sensitive to the correct background intensity level. On most spectral traces this problem could be eliminated by careful evaluation of that level. Also, the scan rate could affect the data if it were too rapid, as pointed out before. Such attenuation was insignificant.

Since such a consistent curvature would arise from a systematic cause, no intermittent effects such as rapid beam current changes or density fluctuations could be blamed. Slow changes in beam current were taken into account by appropriate corrections in the fluorescence output. A few density measurements were conducted primarily to point up what changes in fluorescence could be expected in the course of a tunnel run. That experimental data showed definitely that the density variations were not the cause of bending in the observed points. The condition of the test gas could have given rise to such an apparent deviation of the data from a straight line. A non-Boltzmann distribution of the N_2 ground state or some condition which might alter the theoretical model (condensation, for instance) are possibilities which have not been ruled out experimentally. Further investigation is necessary to substantiate definite conclusions.

RESULTS

Measured Temperature

The measurements obtained in the Langley 12-inch hypersonic ceramic-heated tunnel, by using the electron beam technique, are illustrated by data points in figure 10. Each figure contains results obtained for a range of stagnation pressures at a given stagnation temperature. The stagnation pressures are given in psia units to allow for easy comparison with reference 11. Free-stream static temperature points are the rotational data, as previously indicated. Corresponding vibrational temperatures are given in parentheses. Each circled point is an average over some collection of individual data points. Since each rotational measurement was made by a least-squares fit, a standard deviation could be assigned to each. These deviations were used to weight the temperatures in calculating the average value at any given stagnation condition. The number of measurements represented by a point varied considerably, the least 5 and the most 20. Vibrational temperatures are a simple mean value of one, two, or three individual runs weighted only to the extent that doubtful data (too near the end of the run, for instance) are omitted.

Weighting the average value calculated as the free-stream temperature is appropriate because of the statistical analysis by which an individual measurement could be evaluated. The vibrational measurement with fewer data is subject to larger estimated uncertainties. A simple mean value must then be used. The uncertainties are discussed in the second part of this section.

Variations in the stagnation parameters from one tunnel run at given p_o and T_o values to another tunnel run occurred. That is, for the several runs made at $T_o = 1400^o$ K and $p_o = 2.76 \times 10^6$ N/m^2 (400 psia) as an example, the variation in the stagnation temperature was about $\pm 15^o$ K and in pressure $\pm 1.0 \times 10^5$ N/m^2 (15 psia). The difference noted in the corresponding rotational and vibrational temperatures, however, could not be correlated with those of the stagnation parameters from run to run. Hence, no account has been made in the averages of T_v and T_r for this difference. Also, uncertainties in the average rotational temperatures, calculated as mentioned previously, are smaller than the estimated uncertainties for individual runs. This fact supports the conclusion that the small variations in stagnation conditions are insignificant.

Uncertainties

In considering the uncertainty of an individual temperature measurement, the rotational and vibrational methods are treated separately. For the case of the rotational temperature, several factors enter the determination and, hence, possibly contribute errors. The electron-beam current directly influenced the instantaneous fluorescence level and the output signal. It was continuously monitored during all runs. For most of the data no variation occurred during the rotational scan, whereas for some as much as 2-percent variation was noted. Appropriate corrections were made in the resultant output, a nominal ± 1-percent uncertainty in the temperatures being considered adequate.

The free-stream density, which directly affects any fluorescence measurement of the present sort, could not be measured during all runs. In order to estimate its influence on the temperature results, a total fluorescence detector was utilized during several tunnel runs. (This detector eliminated the vibrational measurement, as mentioned earlier, during those several data periods.) Overall fluctuations were found to be small and contributed an estimated temperature uncertainty of ± 2 percent.

As explained in the discussion of the methods, the slope of a straight line was used to determine the rotational temperature. This slope was calculated by a least-squares fit with weighting factors.

In turn, a standard deviation was calculated for each slope, which fell in the range ± 2 to ± 4 percent. This factor then contributes ± 2 to ± 4 percent to the temperature uncertainty. An overall estimated uncertainty for the rotational temperature is then ± 5 to ± 7 percent. These values are shown as error bars in the figures.

Some of the sources of error are common to both the vibrational and rotational measurements. The fluorescence output being of similar importance to both, the beam current and density fluctuations enter in the same way. The wide slit allowed a much increased signal from the photomultiplier tube and eliminated the problem of noise. That fact, of course, is evident in the discussion of method. One additional factor, rather

offsetting this, was the combined spectral sensitivity for the spectrometer and phototube, an experimentally determined quantity. The uncertainty due to the evaluation of the sensitivity for the system was estimated at ±4 percent.

In addition to these contributing factors, most of the uncertainty develops from the conversion curve for vibrational temperature as a function of intensity ratio. (See figs. 5 and 6.) The transition probabilities required to calculate the conversion factors are approximate, and uncertain by 5 percent or more. Curves such as those in the figures are at least 8 percent uncertain on this account. Attempts to calibrate experimentally to improve this situation were unsuccessful, largely because of the equilibrium condition in a static test gas, which causes increased uncertainty above room temperature (overlapping of bands discussed earlier; see fig. 4(b)). Future improvements in the calibration procedure are possible, although present agreement using the reported probabilities $p(0,1)$ and $p(1,2)$, as illustrated, is good at 300° K. For the vibrational temperature, the overall uncertainty is then approximately ±15 percent.

DISCUSSION

Reference has been made to the original description of the operation of the Langley 12-inch hypersonic ceramic-heated tunnel (ref. 11). Included in that report are values of the many operating parameters; particularly of interest for the present work are the free-stream temperatures. Such calculated free-stream quantities generally depend, as in the case at hand, upon knowledge of stagnation temperature and pressure, pitot pressure, and perhaps heat-transfer rates, or similar properties. On the basis of initial conditions, with a workable theoretical model of the expansion, a complete description of the gas is possible. The electron-beam measurements may be compared with such calculations.

For the given tunnel the free-stream properties were determined originally at the extremes of frozen and equilibrium flow. (The frozen case is extreme in the sense that no relaxation from stagnation conditions was assumed for molecular vibration.) Reference 18 provided the basis for those estimates which are shown as cross-hatched regions in figure 10. The uncertainty in the estimates is indicated by the cross hatching. As can be seen, the free-stream static temperature was not widely different for the two calculated cases. These figures illustrate the proximity of experimental rotational temperatures (equal to translational temperature) with respect to the two extremes. Excepting two points, all the electron beam data fall between the frozen and equilibrium curves. Indeed, by also examining the vibrational temperatures at corresponding stagnation conditions, one finds the same qualitative agreement. (For T_v, the frozen value would be $T_v = T_0$ and the equilibrium value would be $T_v = T_r = T_\infty$.)

There exists, for the temperature data obtained by using the fluorescence technique, general agreement with the aerodynamic calculations. Also, the rotational and vibrational temperatures are consistent. The departure of the two free-stream temperature points above the equilibrium curve in figure 10(c) is not completely explained. It was pointed out before that there was a peculiar curvature in the rotational data (see fig. 9) that was most prominent at these particular stagnation conditions. However, the efforts to explain the curvature and to correlate it with the deviation from predicted temperatures yielded little conclusive evidence. It may be significant that the stagnation conditions for these data tend to produce supersaturated air. Condensation effects however were not definitely established as the cause of curvature.

With the occurrence of nonequilibrium, as exhibited by the large differences between rotational and vibrational temperature, further comparison of the data has been made. A method of determining nonequilibrium effects, to first order, can be found in reference 19. Developed therein is a scheme of using numerical corrections to the frozen flow parameters. The nozzle shape, as expressed in the factor $p_o r/\tan \alpha$, is one specific parameter in the approach. By assuming apparently reasonable values for r and α and using this first-order method, some important conclusions are reached in reference 20 concerning nitrogen relaxation.

To avoid possible inadequacies in directly assuming $p_o r/\tan \alpha$ (such as properly accounting for the boundary layer), figure 11 has been used to determine values of the parameter from experimental knowledge of the vibrational energy and area ratio. (The units of this nozzle shape factor (atmospheres-centimeters) are those of ref. 19.) Thus, by the method of reference 19, from measured T_v values and the area ratio, $p_o r/\tan \alpha$ is given. Based upon that method of evaluation, corrections can be made in the frozen-flow free-stream temperatures. Some of these corrections are then compared with experimental values in figure 12. The following example will illustrate the nonequilibrium analysis.

An example of the nonequilibrium analysis is given in reference 19. From the pitot pressure measurements reported in reference 11, at $p_o = 65$ psia and $T_o = 2050^\circ$ K, $\frac{q}{p_o} = 0.5474 \times 10^{-3}$ where q is the dynamic pressure $\frac{1}{2}\rho V^2$. The vibrational temperature T_v is 1350° K. Then, $\frac{\sigma(T_v)}{\sigma(T_o)} = 0.379$. The area ratio is actually on the asymptotic part of the curves in figure 11, since it is very close to the frozen-flow value given in reference 18 (which corresponds to q/p_o). Then with $\sigma(T_v)/\sigma(T_o)$,

$$\frac{p_o r}{\tan \alpha} \approx 0.9 \times 10^{-3} \text{ atm-cm}$$

With the appropriate correction based on this nozzle parameter, a value of

$$\left(\frac{q}{p_o}\right)_f = 0.549 \times 10^{-3}$$

is found where f indicates frozen flow, or precisely the values of reference 18. Observe that

$$\left(\frac{T_\infty}{T_o}\right)_f = 0.3046 \times 10^{-1}$$

This frozen-flow value must be corrected by using figure 2 of reference 19

$$T'_\infty = \left(\frac{T_\infty}{T_o}\right)_f (\text{Correction factor})(T_o)$$

where T'_∞ is the free-stream temperature in the relaxed flow condition. Then

$$T'_\infty = \left(0.3046 \times 10^{-1}\right)(1.095)(2050^o\ K) = 68.4^o\ K$$

At stagnation condition, that is, $T_o = 2050^o$ K, and $p_o = 65$ psia, the free-stream (and rotational) temperature should be 68.4^o K by this first-order approximate method.

Values of $p_o r/\tan \alpha$ determined as described here appear to be very large. For instance, based upon tunnel geometry, the possible $p_o r/\tan \alpha$ for conditions of the example in the preceding paragraph must be less than 15 atmospheres-centimeters, but the calculation shows about 900 atmospheres-centimeters. Without attempting to develop the details here, reference 19 and other references can be consulted to see that the difference may well be traced to the vibrational relaxation time. Unfortunately, the present reported temperature measurements do not provide a thorough enough set to establish a definite value for the relaxation time.

Further consideration which is possible is illustrated by the two sets of calculated temperatures in figure 12. The points represented by squares were determined by using the same relaxation parameters as in reference 19. There appears to be some difference between nitrogen vibrational relaxation taking place in a pure nitrogen flow and where it occurs in the presence of other gases (that is, in air). Reference 21 presents experimental evidence to this effect. Since the measurements discussed herein took place in an air stream, the second set of points (diamond shaped) where calculated by assuming a more rapid relaxation – about 10 times as fast. It appears that the data are predicted by the basic first-order model for calculation. However, no exact value of the relaxation time could be determined within the limits of these measurements.

Recently, a rather large research effort has been concerned with the problem of relaxation, and other related effects such as dissociative nonequilibrium and radiative transfer. References 22, 23, 24, and the previous ones illustrate that fact. Although a detailed discussion has been avoided in the present work, some indication of the problem of flow analysis has been attempted. The use of the electron-beam technique as a diagnostic tool has been illustrated, and several free-stream temperature measurements reported.

CONCLUSIONS

An electron-beam fluorescence technique has been employed to measure free-stream nitrogen rotational and vibrational temperatures in air at the Langley 12-inch hypersonic ceramic-heated tunnel. This work included establishing the sources of measurement uncertainty and minimizing their effect on the temperature measurements. On the basis of this investigation the following conclusions are made:

1. A preliminary laboratory investigation, especially concerned with developing the vibrational temperature measurement, has been described. Use of the integrated P-branch intensity provided a rather straightforward method to determine the required band intensity ratio. Comparison with the theoretical ratio as a function of temperature was made. Consistent data interpretation required that a choice be made between different values of transition probabilities reported, particularly $p(0,0)$, $p(0,1)$, and $p(1,2)$. An experimental evaluation of $p(1,3)$ was necessary.

2. To improve upon the visual determination, a least-squares analysis was used to find the best linear fit for each set of rotational-line intensity data. For expedience, this procedure was developed and programed on a computer for the specific temperature range encountered in this work. This procedure should be the best solution when only random displacements from the true straight line are expected.

3. Nitrogen rotational and vibrational temperatures were measured in the free stream of the Langley 12-inch hypersonic ceramic-heated tunnel. The range of the rotational (hence, translational) temperature was 39° K to 72° K. Corresponding vibrational temperatures were found to be 850° K to 1320° K. The points measured are shown.

4. Uncertainties were evaluated for each of the measured quantities. For rotational measurements, the estimated uncertainty is ± 5 to ± 7 percent, depending on the individual case. Vibrational temperatures were about ± 15 percent uncertain. It has been ascertained that further investigation may improve this latter figure.

5. All the rotational data accumulated did not seem to fit a straight line as expected. This problem was examined with respect to the possible systematic errors which might have occurred. It was not traced to a definite source.

6. Finally, reasonable agreement between these measurements and aerodynamic predictions was obtained. In addition to examining the extreme equilibrium and strictly frozen-flow cases, a first-order relaxing model provides some additional comparison. The present data partially follows the nonequilibrium calculation when a relaxation about 10 times as fast as that of NASA TN D-1810 is assumed.

7. Some investigators have found disagreement between measured rotational temperatures and calculated or measured reference translational temperatures. The possibility of correcting electron beam temperature measurements has been omitted from this report because calibration has not been possible at the low temperatures and, further, there are wide differences in estimates of the magnitude of such a correction and its physical basis. Additionally, direct comparison of present results with the calculations appears to be favorable.

Langley Research Center,
National Aeronautics and Space Administration,
Langley Station, Hampton, Va., July 3, 1968,
125-24-03-22-23.

REFERENCES

1. Muntz, E. P.: Measurement of Rotational Temperature, Vibrational Temperature, and Molecular Concentration, in Non-Radiating Flows of Low Density Nitrogen. Rept. No. 71 (AFOSR TN 60-499), Inst. Aerophys., Univ. of Toronto, Apr. 1961.

2. Sebacher, Daniel I.; and Duckett, Roy J.: A Spectrographic Analysis of a 1-Foot Hypersonic-Arc-Tunnel Airstream Using an Electron Beam Probe. NASA TR R-214, 1964.

3. Robben, F.; and Talbot, L.: Measurements of Rotational Temperatures in a Low-Density Wind Tunnel. Phys. Fluids, vol. 9, no. 4, Apr. 1966, pp. 644-652.

4. Petrie, S. L.; Pierce, G. A.; and Fishburne, E. S.: Analysis of the Thermo-Chemical State of an Expanded Air Plasma. Tech. Rept. No. AFFDL-TR-64-191, Ohio State Univ. Res. Found., Aug. 1965.

5. Hunter, William Winslow, Jr.: Measurement of $N_2X^1\Sigma g^+$ Rotational and Vibrational Temperatures Over a 300^o K to 1100^o K Range Using a High-Energy Electron Beam. M.A. Thesis, The College of William and Mary, 1965.

6. Bennet, R. G.; and Dalby, F. W.: Experimental Determination of the Oscillator Strength of the First Negative Bands of N_2^+. J. Chem. Phys., vol. 31, no. 2, Aug. 1959, pp. 434-441.

7. Bates, D. R., ed.: Atomic and Molecular Processes. Academic Press, 1962, pp. 47-78, 374-420.

8. Herzberg, Gerhard: Molecular Spectra and Molecular Structure. I. Spectra of Diatomic Molecules, Second ed., D. Van Nostrand Co., Inc., c.1950.

9. Cottrell, T. L.; and McCoubrey, J. C.: Molecular Energy Transfer in Gases. Butterworth & Co. Ltd., c.1961.

10. Brout, Robert: Rotational Energy Transfer in Diatomic Molecules. J. Chem. Phys., vol. 22, no. 7, July 1954, pp. 1189-1190.

11. Clark, Louis E.: Description and Initial Calibration of the Langley 12-Inch Hypersonic Ceramic-Heated Tunnel. NASA TN D-2703, 1965.

12. Allen, R. A.: Nonequilibrium Shock Front Rotational, Vibrational and Electronic Temperature Measurements. J. Quart. Spectrosc. Radiat. Transfer, vol. 5, no. 3, May/June 1965, pp. 511-523.

13. Clark, K. C.; and Belon, A. E.: Spectroscopic Observations of the Great Aurora of 10 February 1958-I Abnormal Vibration of N_2^+. J. Atmos. Terrest. Phys., vol. 16, nos. 3/4, Nov. 1959, pp. 205-219.

14. Reis, Victor H.: Oscillator Strengths for the N_2 Second Positive and N_2^+ First Negative Systems From Observations of Shock Layers About Hypersonic Projectiles. J. Quart. Spectry. Radiat. Transfer, vol. 4, no. 6, Nov./Dec. 1964, pp. 783-792.

15. Wallace, L. V.; and Nicholls, R. W.: The Interpretation of Intensity Distributions in the N_2 Second Positive and N_2^+ First Negative Band Systems. J. Atmos. Terrest. Phys. (Res. Notes), vol. 7, nos. 1/2, Aug. 1955, pp. 101-105; J. Atmos. Terrest. Phys. (Errata), vol. 24, Aug. 1962, p. 749.

16. Shepherd, G. G.; and Hunten, D. M.: On the Measurement of Rotational Temperature From Resolved Auroral Nitrogen Bands. J. Atmos. Terrest. Phys., vol. 6, no. 6, June 1955, pp. 328-335.

17. Topping, J.: Errors of Observation and Their Treatment. Reinhold Pub. Corp., 1960.

18. Ames Research Staff: Equations, Tables, and Charts for Compressible Flow. NACA Rep. 1135, 1953. (Supersedes NACA TN 1428.)

19. Erickson, Wayne D.: Vibrational-Nonequilibrium Flow of Nitrogen in Hypersonic Nozzles. NASA TN D-1810, 1963.

20. Sebacher, Daniel I.: An Electron Beam Study of Vibrational and Rotational Relaxing Flows in Nitrogen and Air. Proceedings of the 1966 Heat Transfer and Fluid Mechanics Institute, Michel A. Saad and James A. Miller, eds., Stanford Univ. Press, c.1966, pp. 315-334.

21. White, Donald R.; and Millikin, Roger C.: Vibrational Relaxation in Air. AIAA J., vol. 2, no. 10, Oct. 1964, pp. 1844-1846.

22. Clarke, J. F.; and McChesney, M.: The Dynamics of Real Gases. Butterworths, 1964.

23. Millikan, Roger C.; and White, Donald R.: Systematics of Vibrational Relaxation. J. Chem. Phys., vol. 39, no. 12, Dec. 15, 1963, pp. 3209-3213.

24. Hurle, I. R.; Russo, A. L.; and Hall, J. Gordon: Spectroscopic Studies of Vibrational Nonequilibrium in Supersonic Nozzle Flows. J. Chem. Phys., vol. 40, no. 8, 15 Apr. 1964, pp. 2076-2089.

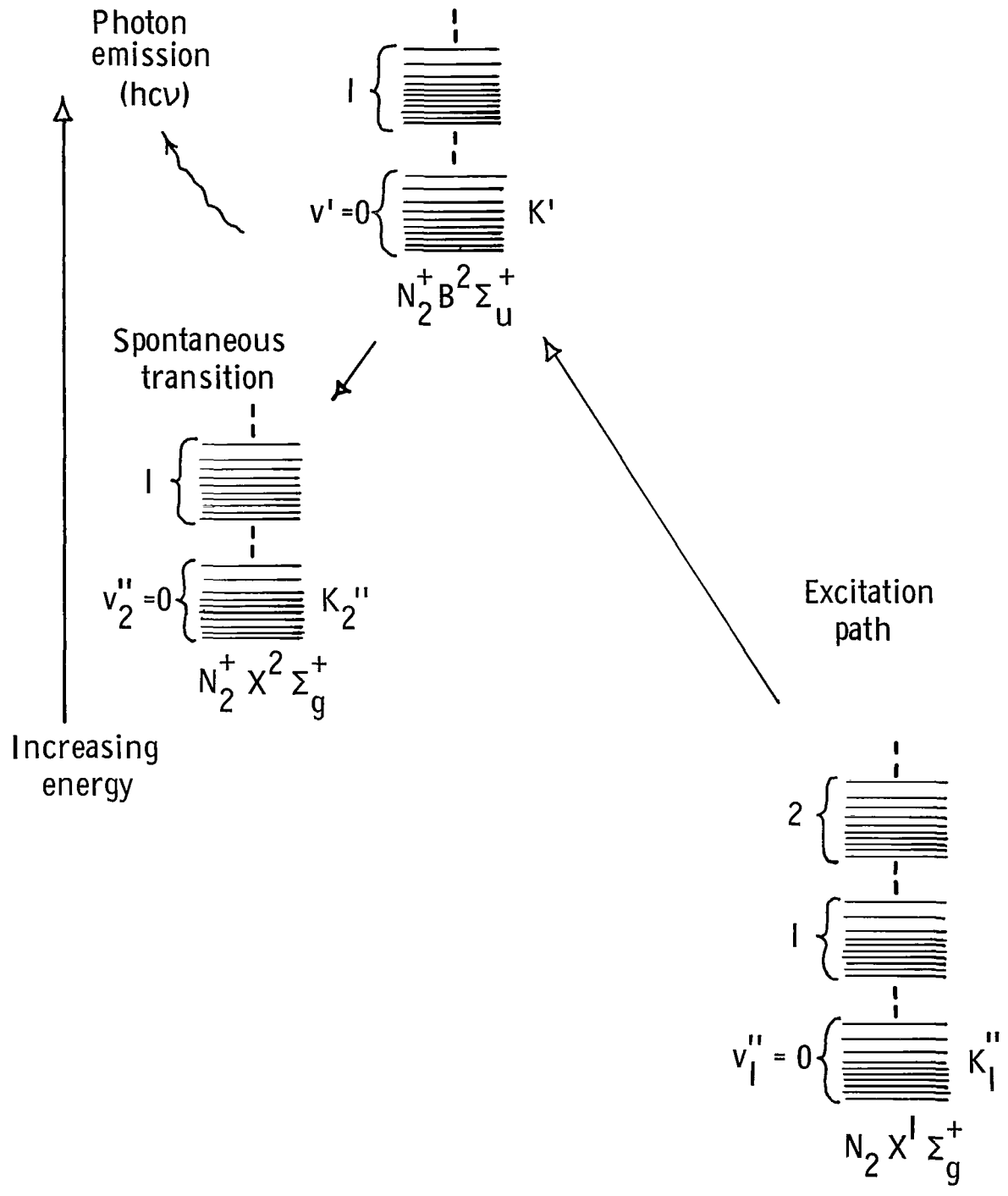

Figure 1.- Schematic energy level diagram of N_2.

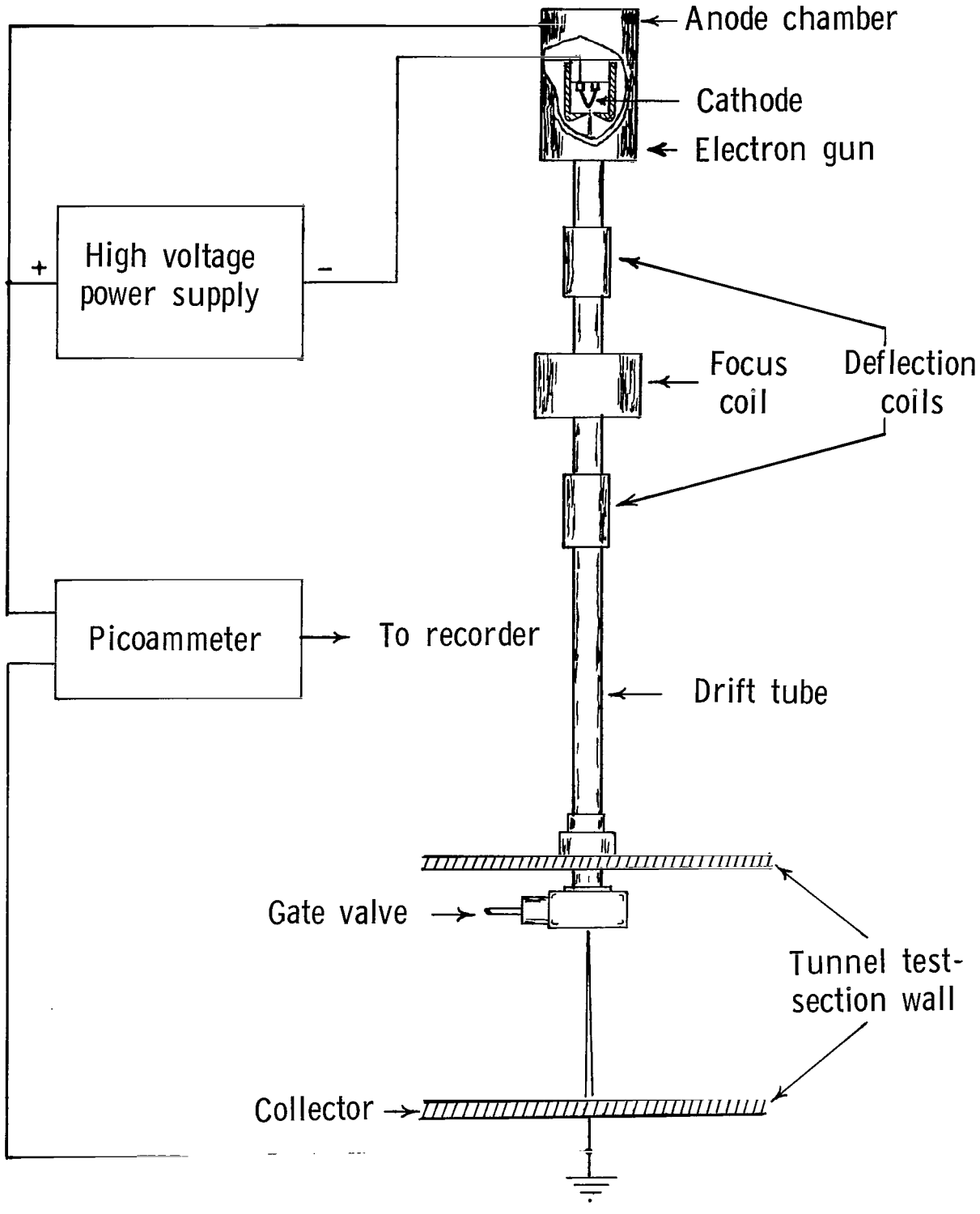

Figure 2.- Electron gun installation.

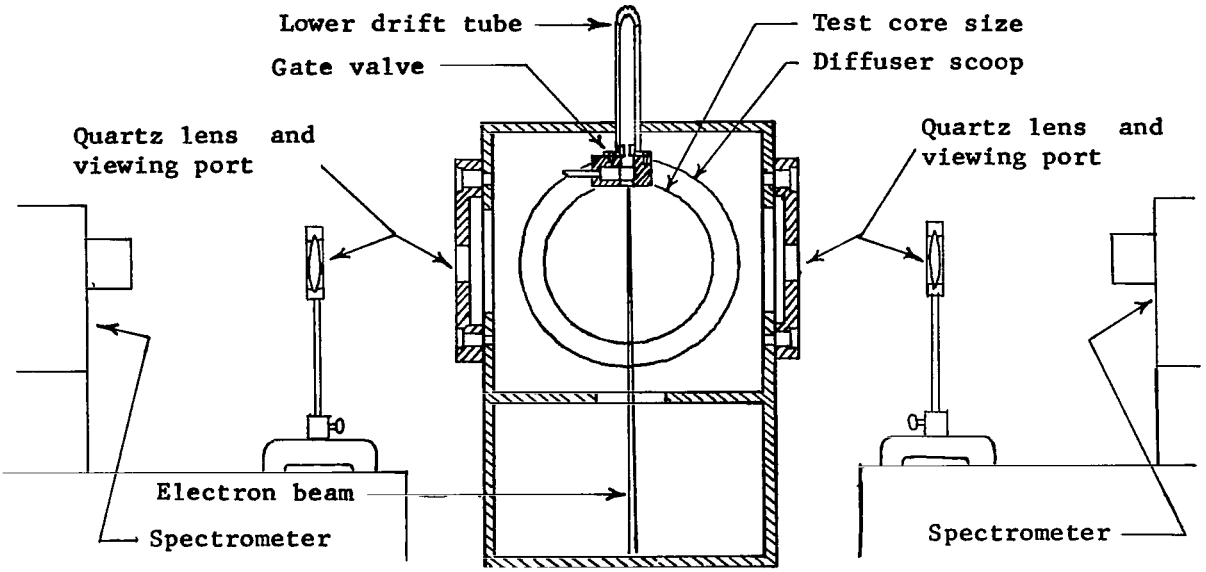

End view

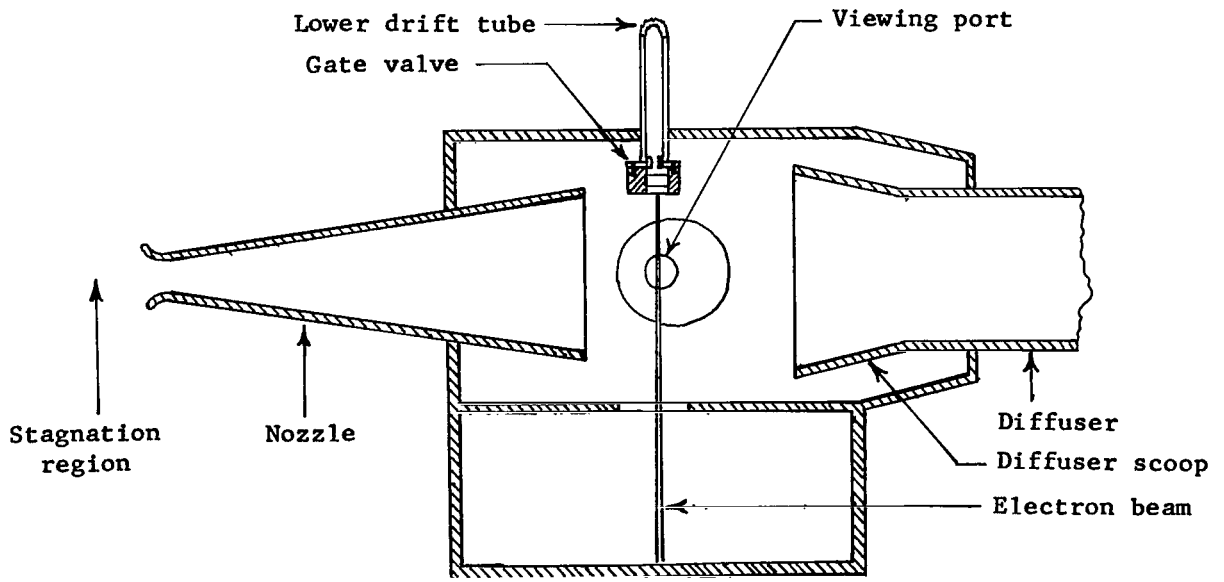

Side view

Figure 3.- Gun and optics placement at Langley 12-inch hypersonic ceramic-heated tunnel.

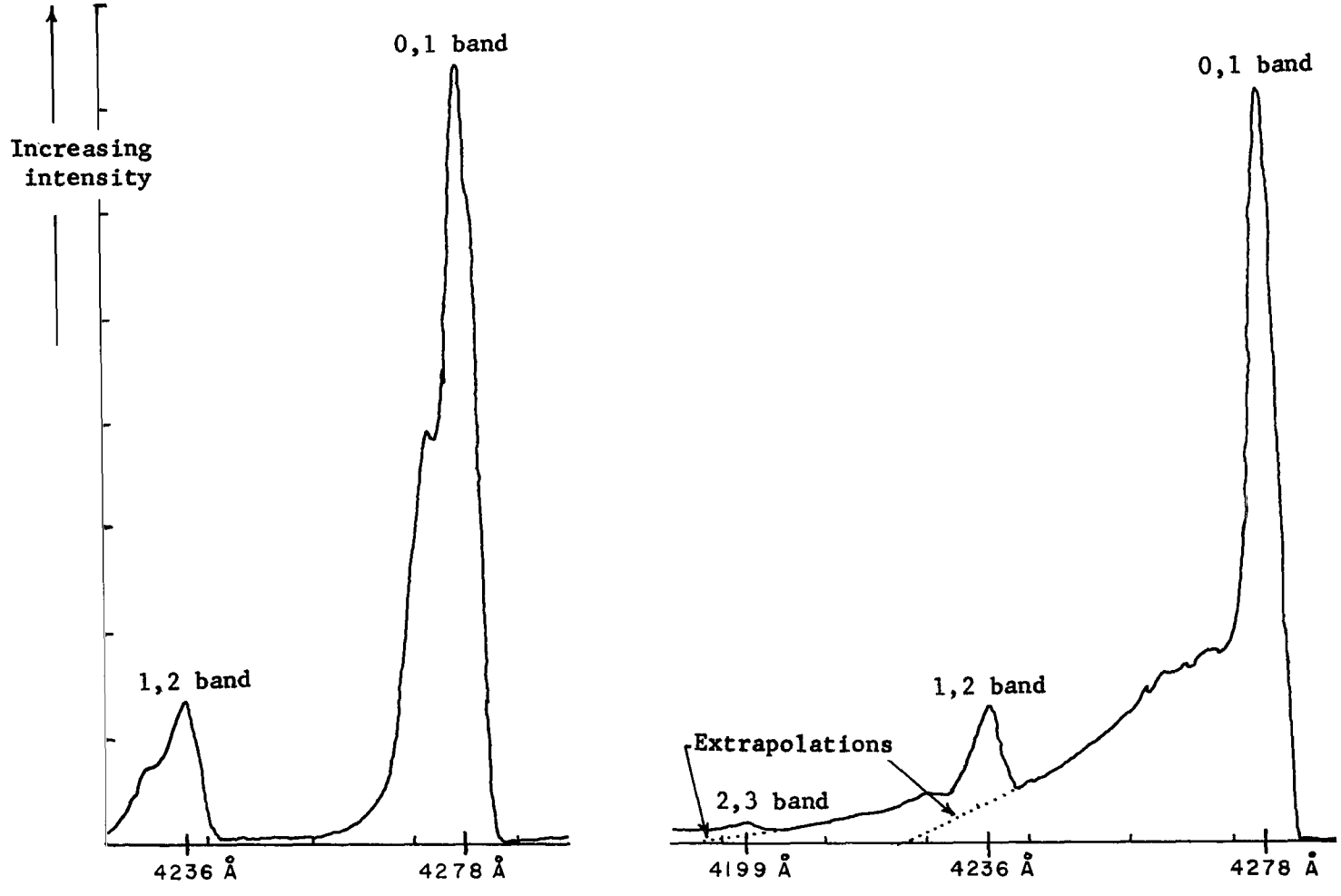

(a) Tunnel results. Stagnation parameters: $T_{0_2} = 1810^0$ K; and $p_0 = 415$ psia (2.86×10^6 N/m2).

(b) Static test data. ($T_r = T_v = T_\infty$.) Reference temperature, 914^0 K.

Figure 4.- Observed vibrational spectra of $N_2^+\left(B^2\Sigma_u^+ \rightarrow X^2\Sigma_g^+\right)$.

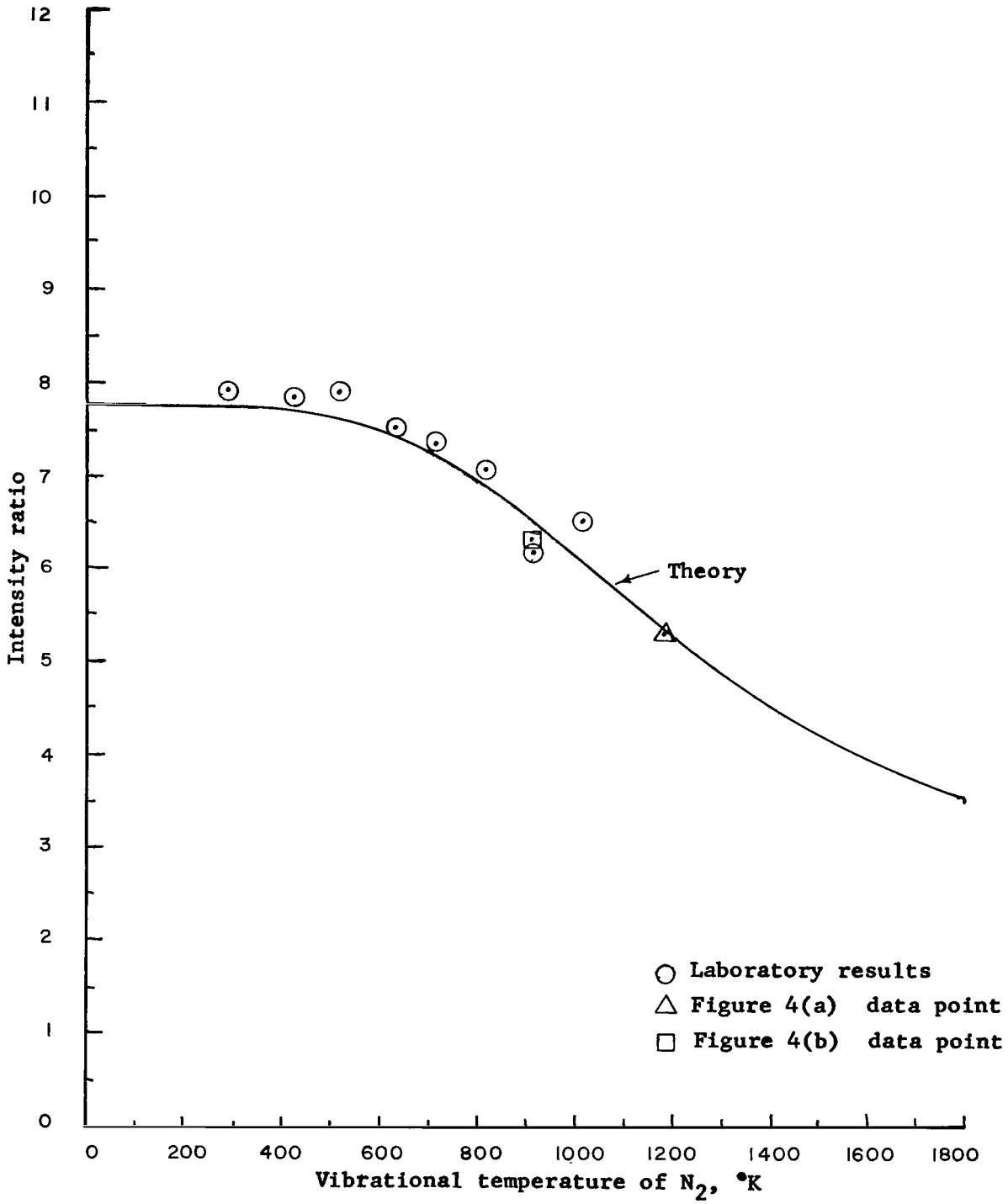

Figure 5.- Theoretical and observed temperature dependence of $I_{0,1}/I_{1,2}$.

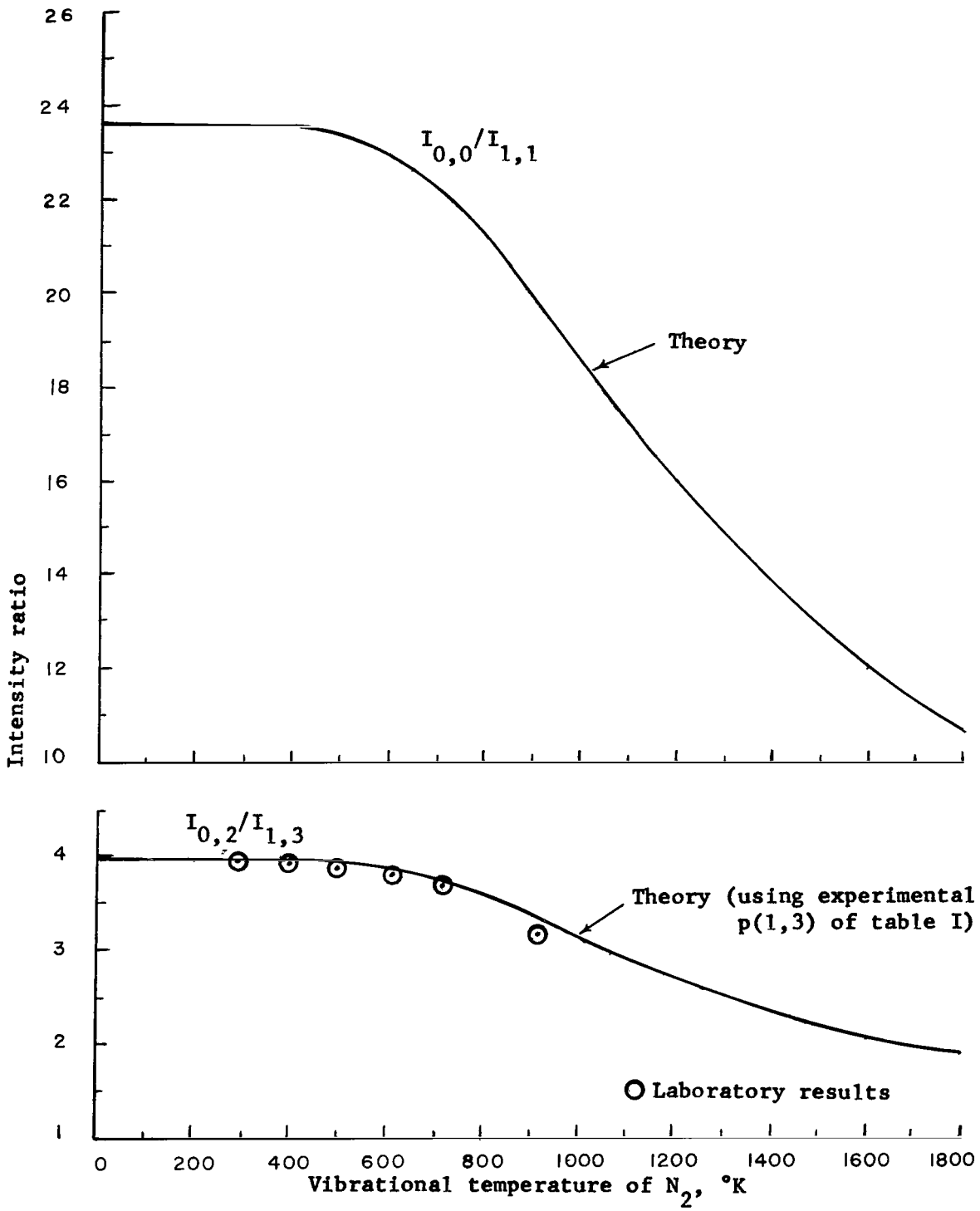

Figure 6.- Theoretical temperature dependence of $I_{0,2}/I_{1,3}$ and $I_{0,0}/I_{1,1}$.

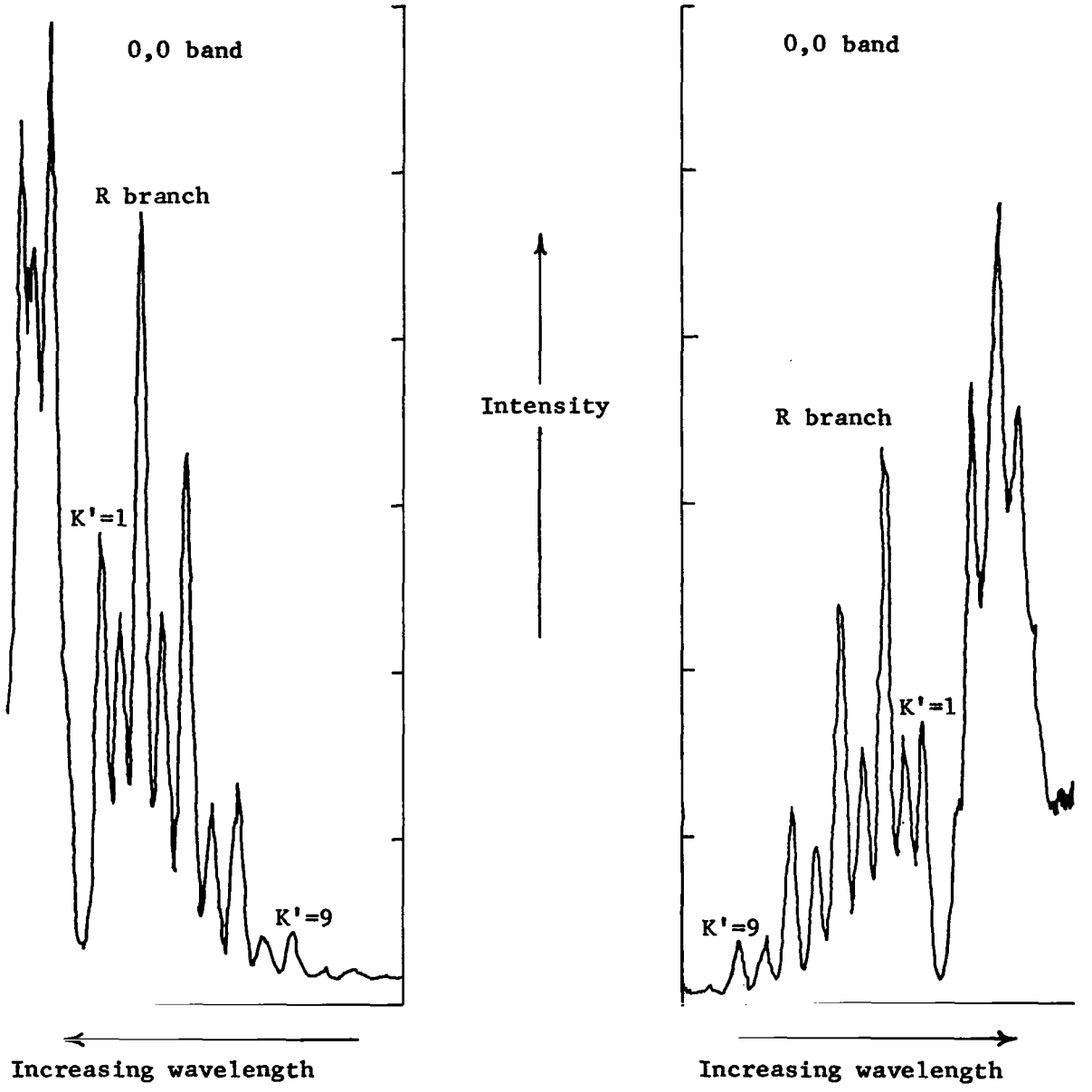

(a) Rotational temperature, 61.9° K; stagnation conditions: T_0 = 2050° K; p_0 = 215 psia (1.48×10^6 N/m^2).

(b) Rotational temperature, 50.6° K; stagnation conditions: T_0 = 1816° K; p_0 = 215 psia (1.48×10^6 N/m^2).

Figure 7.- Rotational spectra data observed in free stream of Langley 12-inch hypersonic ceramic-heated tunnel.

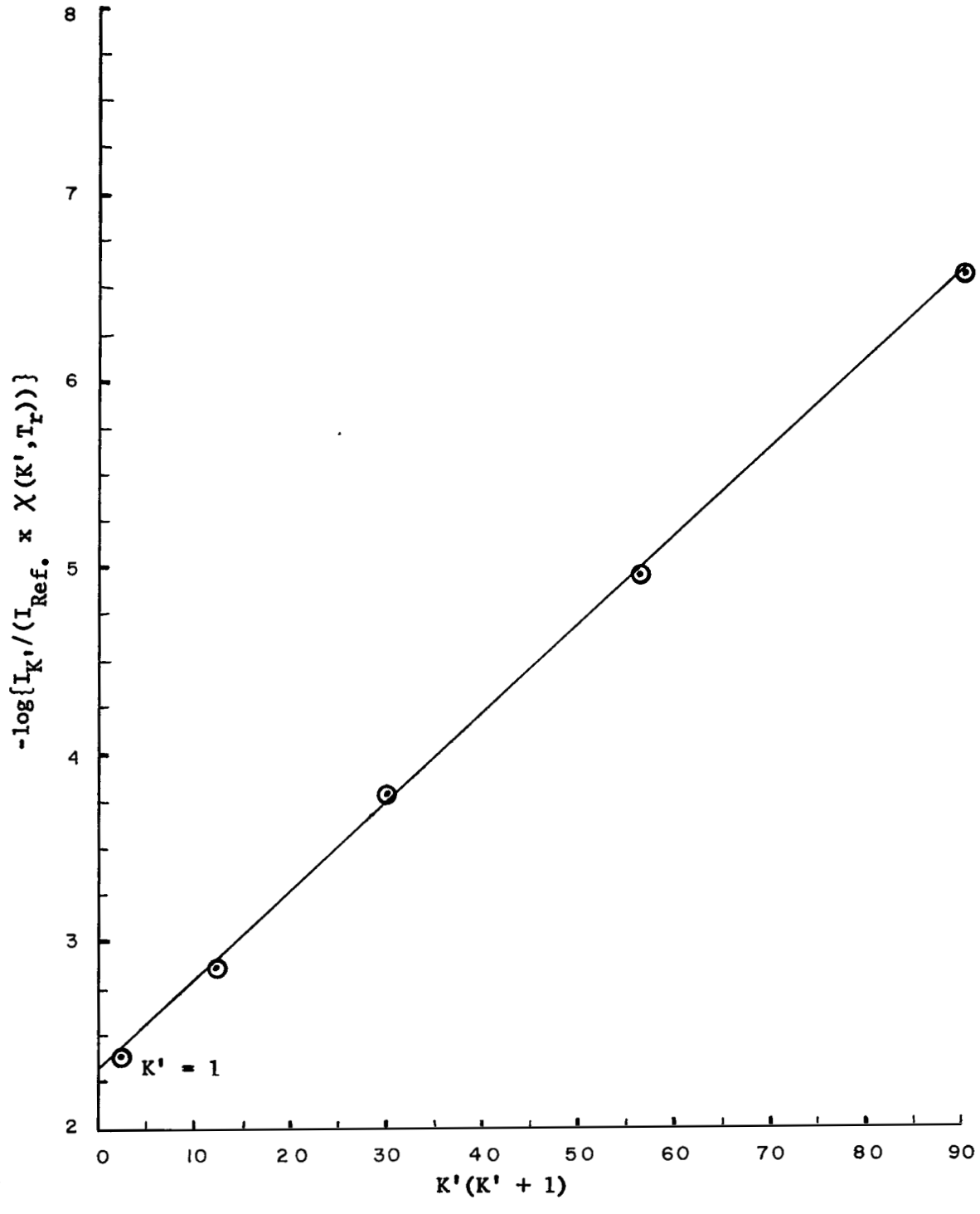

Figure 8.- Tunnel data. Slope = 0.468×10^{-1}; $T_r = 619^0$ K; $T_0 = 2050^0$ K; $p_0 = 215$ psia $\left(1.48 \times 10^6 \text{ N/m}^2\right)$.

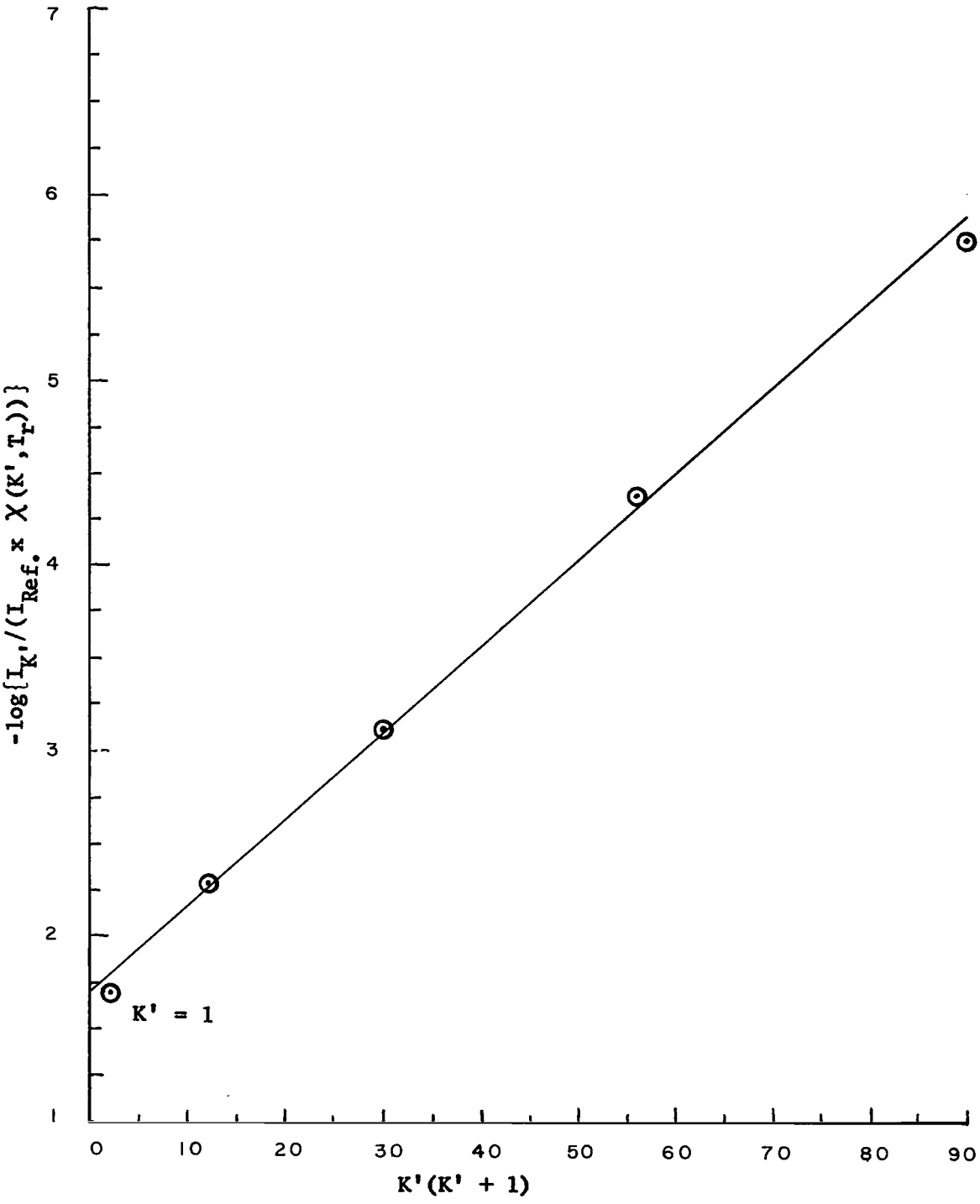

(a) $T_r = 60.5^0$ K; $T_0 = 1816^0$ K; $p_0 = 80$ psia $(0.55 \times 10^6$ N/m$^2)$.

Figure 9.- Rotational temperature determination illustrating slight curvature observed.

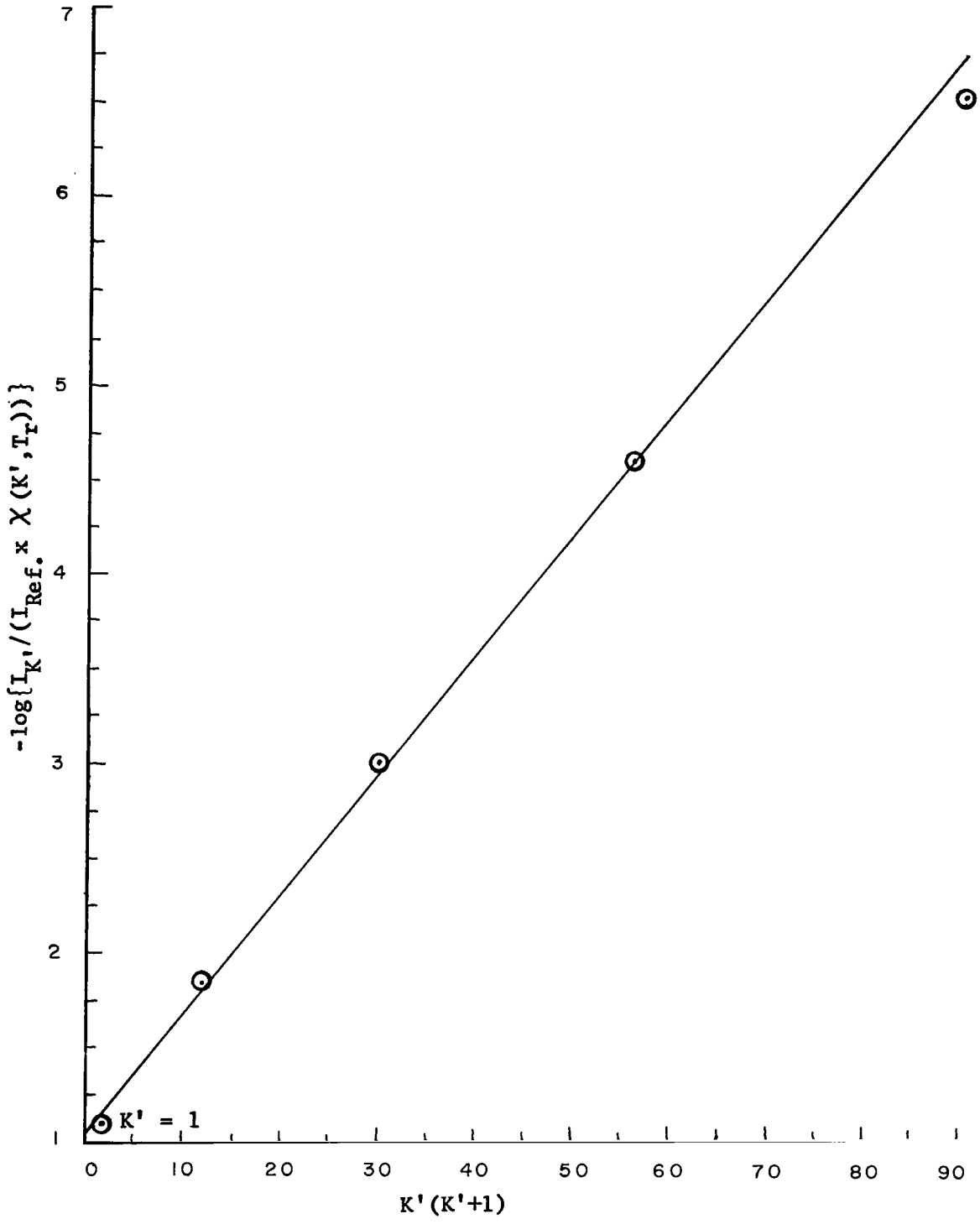

(b) $T_r = 45.2^0$ K; $T_0 = 1385^0$ K; $p_0 = 75$ psia $(0.52 \times 10^6$ N/m$^2)$.

Figure 9.- Concluded.

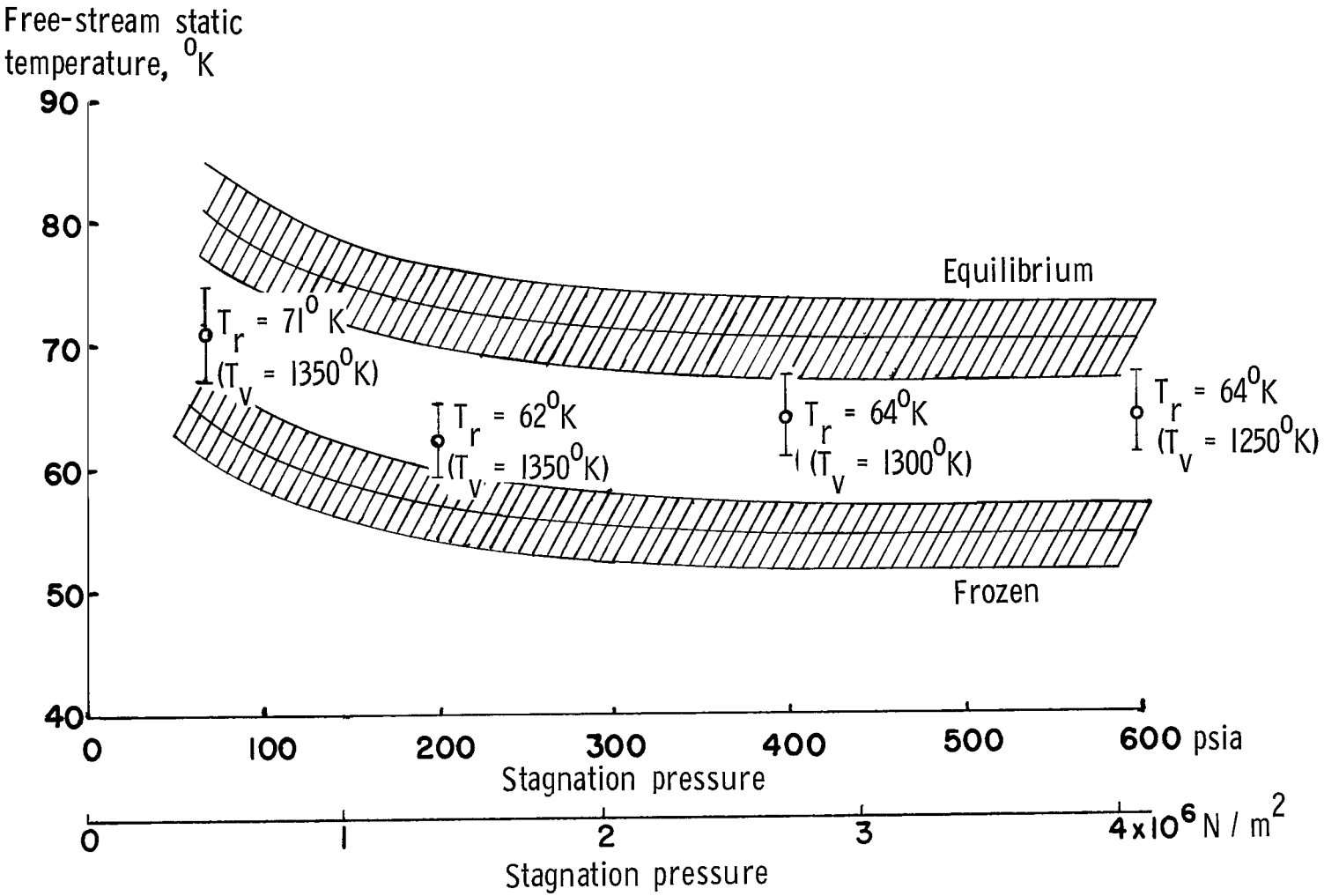

(a) Stagnation temperature, 2050^{0} K.

Figure 10.- Results of temperature measurements conducted in the Mach 13, Langley 12-inch hypersonic ceramic-heated tunnel.

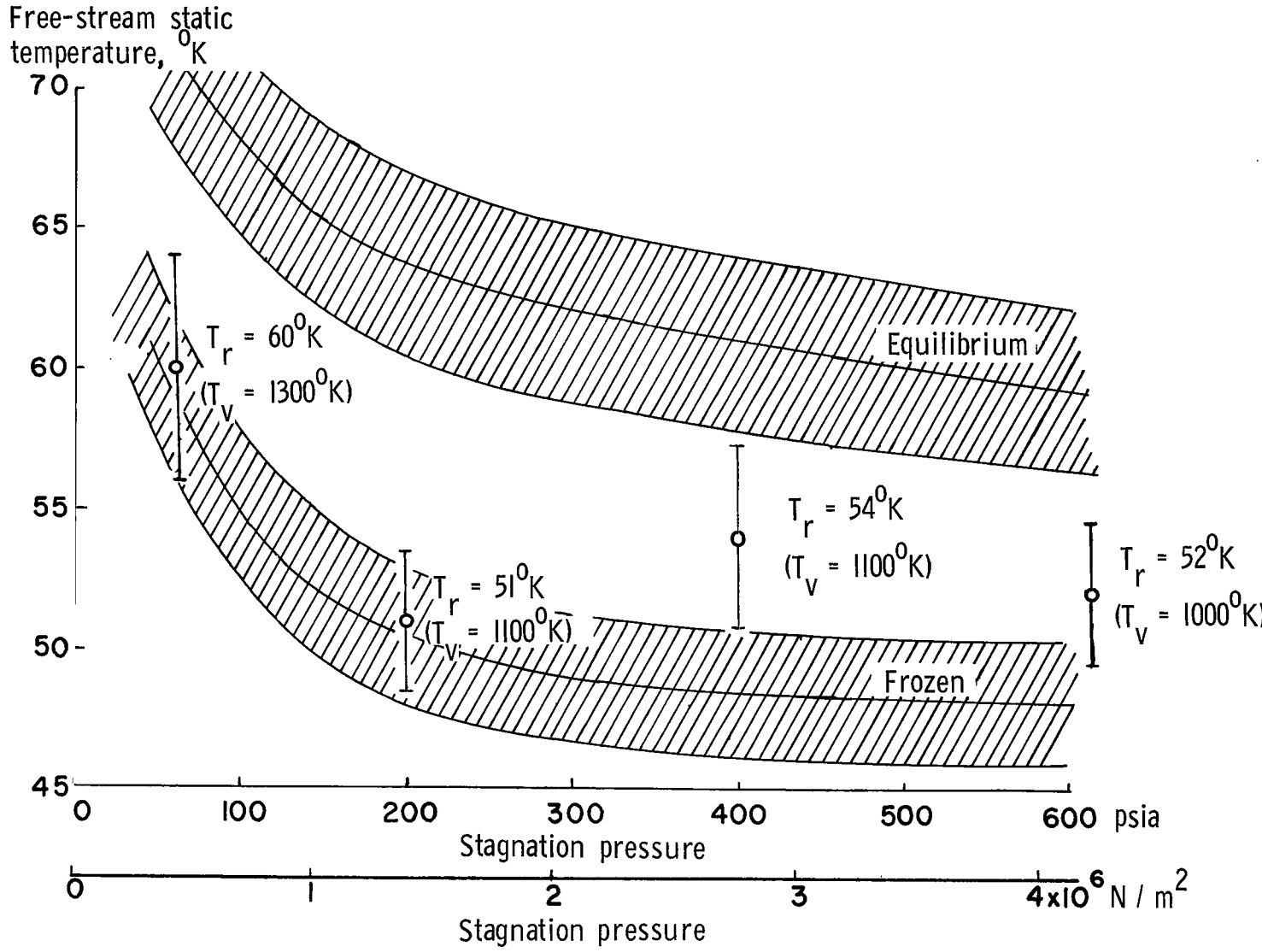

(b) Stagnation temperature, 1800° K.

Figure 10.- Continued.

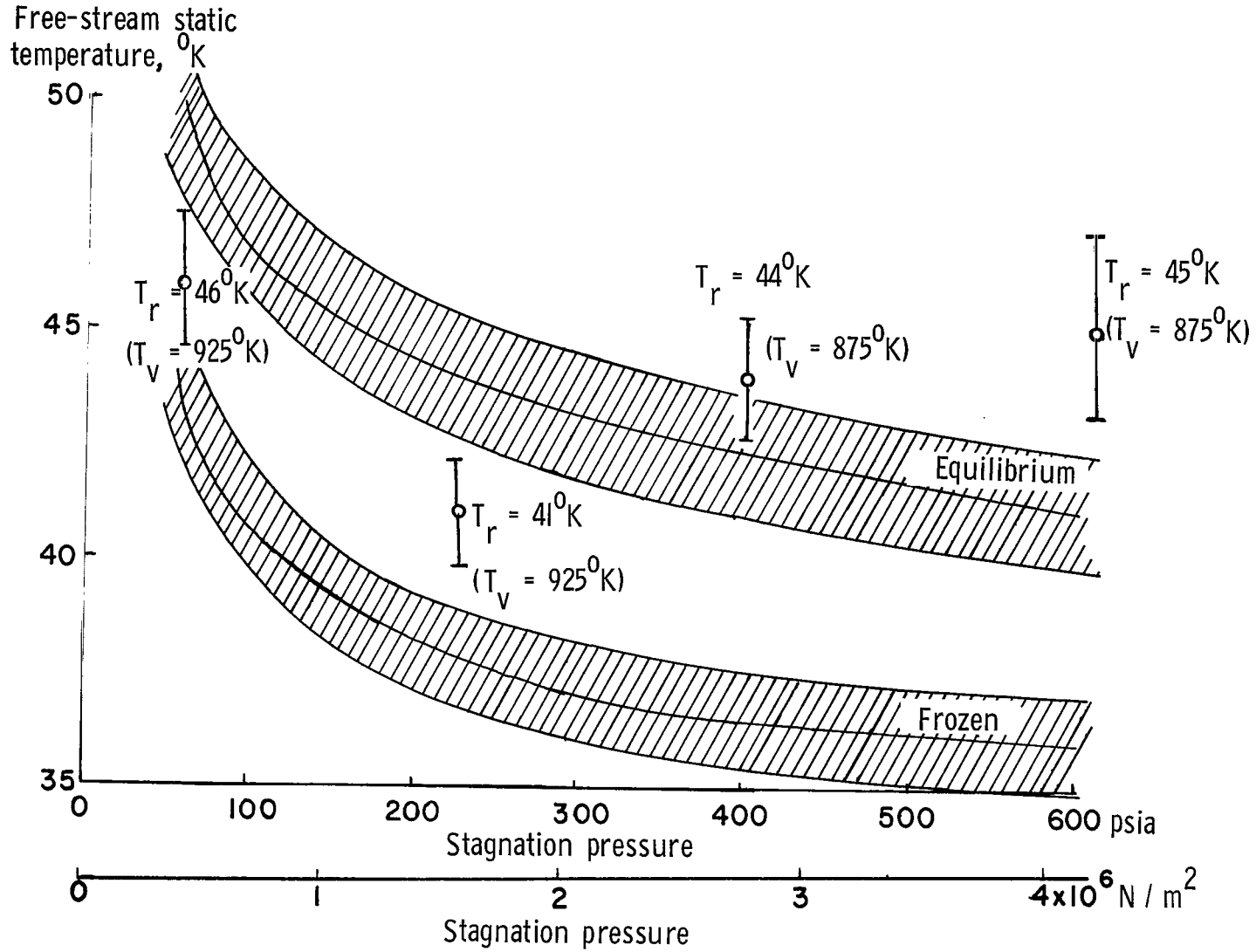

(c) Stagnation temperature, 1380° K.

Figure 10.- Concluded.

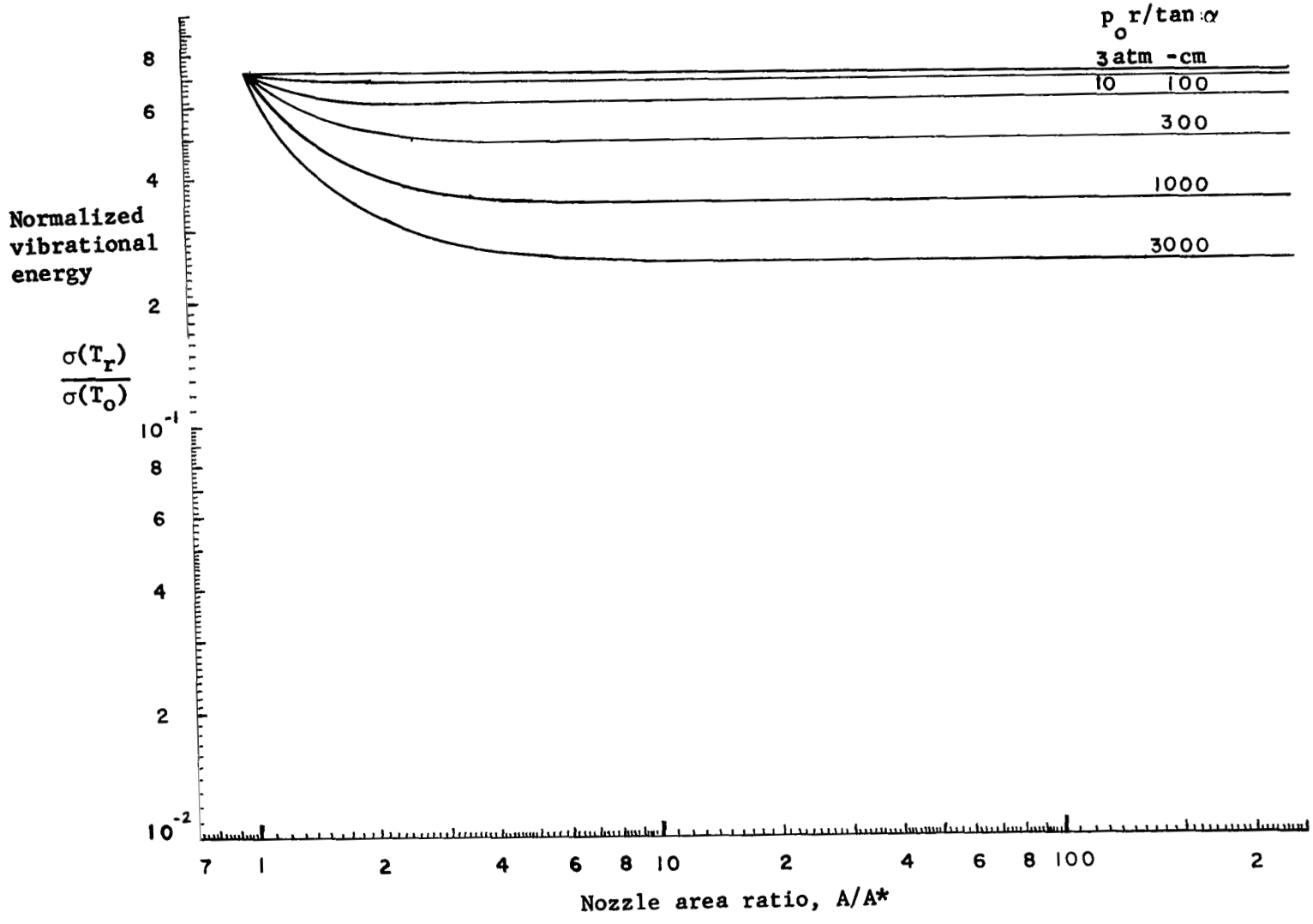

Figure 11.- Vibrational energy as a function of area ratio for $T_0 = 2000^0$ K and various $p_0 r/\tan\alpha$.

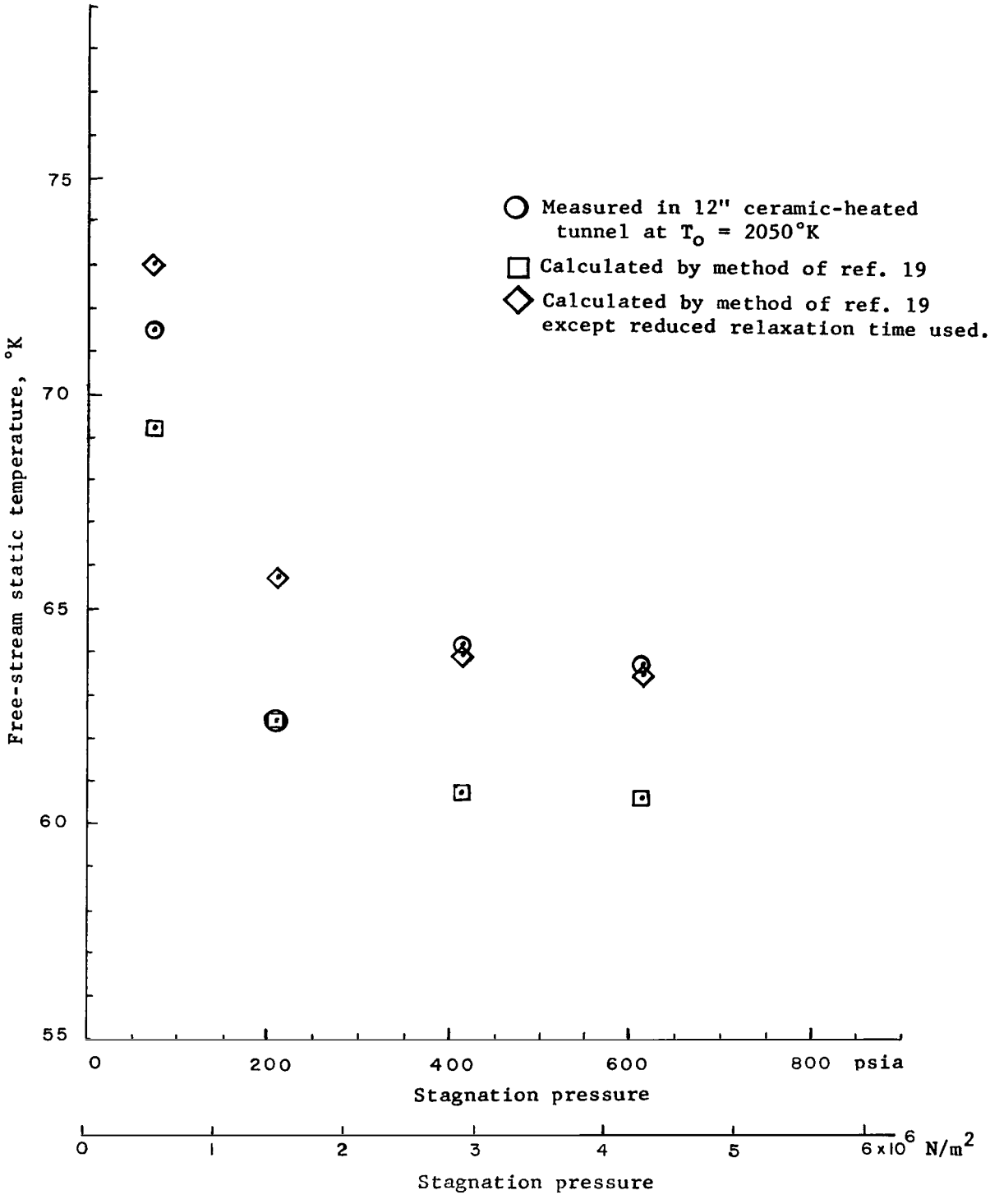

Figure 12.- Comparison of free-stream translational temperature for $T_0 = 2050^0$ K.

"The aeronautical and space activities of the United States shall be conducted so as to contribute . . . to the expansion of human knowledge of phenomena in the atmosphere and space. The Administration shall provide for the widest practicable and appropriate dissemination of information concerning its activities and the results thereof."

—NATIONAL AERONAUTICS AND SPACE ACT OF 1958

NASA SCIENTIFIC AND TECHNICAL PUBLICATIONS

TECHNICAL REPORTS: Scientific and technical information considered important, complete, and a lasting contribution to existing knowledge.

TECHNICAL NOTES: Information less broad in scope but nevertheless of importance as a contribution to existing knowledge.

TECHNICAL MEMORANDUMS: Information receiving limited distribution because of preliminary data, security classification, or other reasons.

CONTRACTOR REPORTS: Scientific and technical information generated under a NASA contract or grant and considered an important contribution to existing knowledge.

TECHNICAL TRANSLATIONS: Information published in a foreign language considered to merit NASA distribution in English.

SPECIAL PUBLICATIONS: Information derived from or of value to NASA activities. Publications include conference proceedings, monographs, data compilations, handbooks, sourcebooks, and special bibliographies.

TECHNOLOGY UTILIZATION PUBLICATIONS: Information on technology used by NASA that may be of particular interest in commercial and other non-aerospace applications. Publications include Tech Briefs, Technology Utilization Reports and Notes, and Technology Surveys.

Details on the availability of these publications may be obtained from:

SCIENTIFIC AND TECHNICAL INFORMATION DIVISION

NATIONAL AERONAUTICS AND SPACE ADMINISTRATION

Washington, D.C. 20546